

Microscopic Study of Deformed Neutron-Deficient $^{124-132}\text{Ce}$ Isotopes

R.K. Bhat, Rani Devi, and S.K. Khosa

Department of Physics and Electronics

University of Jammu, 180006, India

Received on 11 October, 2002

Variation after Projection (VAP) calculations in conjunction with Hartree Bogoliubov (HB) ansatz have been carried out for $^{124-132}\text{Ce}$ mass chain. In this framework, the yrast spectra, B(E2) transition probabilities and occupation numbers for various shell model orbits have been obtained. The observed decrease in deformation in going from ^{124}Ce to ^{132}Ce is seen to arise due to a slow decrease in the occupation of $1g_{7/2}$ proton orbit and a systematic increase in the occupations of $2d_{5/2}$, $1g_{7/2}$ and $1h_{11/2}$ neutron orbits. Besides this, the experimental low-lying yrast spectra and B(E2) transition probabilities are reproduced with reasonable accuracy by using PQOH interaction.

I Introduction

An inspection of the recent experimental data [1-10], for example the energy level spacings and the lifetimes of excited states in the light neutron-deficient Cerium (Ce) nuclei reveals a region of pronounced collective behavior. The experimental data [1-5] shows that this collective pattern evolves rapidly in moving from ^{132}Ce to ^{130}Ce to ^{128}Ce . Sometime ago, Zhang et al. [11] pointed out that E_4^+/E_2^+ ratio is an important parameter for determining the shape of a nucleus. For a rigid rotator its value should be 3.33 while as its value for spherical nucleus should be around 2. The values in between these two limits indicate that the nucleus is quasi-deformed and has vibrational character. As one moves away from ^{132}Ce towards the lower mass side, one observes a systematic decrease in the energy value of 2^+ state and a systematic increase in the value of the ratio of E_4^+/E_2^+ . For example, the values of E_2^+ and E_4^+/E_2^+ for ^{132}Ce are 0.32 MeV and 2.66 and for the lightest ^{124}Ce isotope these values are 0.14 MeV and 3.21, respectively. It may be noted from Table 1 that $^{124-128}\text{Ce}$ are reasonably well deformed nuclei. Sometime back, Lister et al. [9] have predicted lightest Ce isotopes to be axially symmetric rotors with quadrupole deformation $\beta_2 \approx 0.3$. This work reports major advance in knowledge of A=130 region of deformation. They have also said that their work is required to understand the details of the behavior of these nuclei.

A few theoretical attempts [2,9,12] have been made to study the neutron-deficient Ce isotopes. Yan et al. [12] have calculated only the deformation parameters (β , γ) from the decay properties and the energies by using triaxial rotor model for the $^{128-136}\text{Ce}$ isotopes. They found that the calculated parameters are in good agreement with one another. Todd et al.[2] have interpreted the experimental results in ^{130}Ce in terms of the Cranked-shell model by assuming a

prolate deformation with $\epsilon_2 \approx 0.25$. They interpreted the reduced frequency of the highest state observed in ^{130}Ce (26^+) as an effect of $h_{11/2}$ neutron alignment process. It has been found that theoretical attempts have been made by many authors to study specific nuclei and there is a lack of microscopic calculation to study the low-lying systematics of the entire neutron-deficient part of Ce isotopic mass chain in a single framework. It is with this motivation to study the low-lying systematics of the neutron-deficient isotopes that we plan to study these nuclei in a suitable calculational framework.

In the present paper an attempt has been made to carry out a microscopic study of the yrast states and B(E2) transition probabilities in the neutron-deficient $^{124-132}\text{Ce}$, by employing the VAP [13] formalism in conjunction with the HB [14] ansatz for the axially symmetric wave functions. For the calculation of yrast levels, the pairing plus-quadrupole-quadrupole- plus- octupole-octupole plus- hexadecapole-hexadecapole (PQOH) model of effective interaction in a valence space spanned by $3s_{1/2}$, $2d_{3/2}$, $2d_{5/2}$, $2f_{7/2}$, $1g_{7/2}$, $1h_{9/2}$, $1h_{11/2}$ and $1i_{13/2}$ orbits for protons as well as neutrons is employed. The ^{100}Sn is considered as an inert core.

II Computational details

II.1 The one and two body parts of the Hamiltonian

The spherical single-particle energies (S.P.E.'s) that we have employed are (in MeV): $(2d_{5/2}) = 0.0$, $(3s_{1/2}) = 1.4$, $(2d_{3/2}) = 2.0$, $(1g_{7/2}) = 4.0$, $(1h_{11/2}) = 6.5$, $(2f_{7/2}) = 13.0$, $(1h_{9/2}) = 14.0$ and $(1i_{13/2}) = 15.5$. The S.P.E.'s of $2d_{5/2}$, $3s_{1/2}$, $2d_{3/2}$, $1g_{7/2}$ and $1h_{11/2}$ are nearly the same as that employed by Vergados and Kuo [15] as well as

Table 1. The experimental values of the excitation energy of the E_2^+ state, E_4^+/E_2^+ ratio and the intrinsic quadrupole moments of the HB states in $^{124-132}\text{Ce}$ isotopes. Here $\langle Q_0^2 \rangle_\pi$ ($\langle Q_0^2 \rangle_\nu$) give the contribution of the protons (neutrons) to the total intrinsic quadrupole moments. The quadrupole moments have been computed in units of b^2 , where $b = \sqrt{\hbar/m\omega}$ is the oscillator parameter.

Nucleus	E_2^+ Exp.	E_2^+ Th.	E_4^+/E_2^+ Exp.	$\langle Q_0^2 \rangle_{HB}$	$\langle Q_0^2 \rangle_\pi$	$\langle Q_0^2 \rangle_\nu$
^{124}Ce	0.14	0.15	3.21	94.50	40.55	53.95
^{126}Ce	0.17	0.16	3.06	93.83	40.13	53.70
^{128}Ce	0.20	0.17	3.00	91.42	40.00	51.42
^{130}Ce	0.25	0.20	2.84	85.52	39.52	46.00
^{132}Ce	0.32	0.25	2.66	77.80	39.64	38.16

Federman and Pittel [16]. The S.P.E.'s of $2f_{7/2}$, $1h_{9/2}$ and $1i_{13/2}$ orbits are taken from Nilsson diagrams, published in the book by Nilsson and Ragnarsson [17] with small variations so as to reproduce shell closures for $N=82$ for ^{140}Ce .

The two body effective interaction that has been employed is of PQOH type. The pairing plus quadrupole-quadrupole (PQ) interaction is of the type given in reference [18]. The pairing part can be written as

$$V_P = (G/4) \sum_{\alpha\beta} S_\alpha S_\beta a_\alpha^\dagger a_{\bar{\alpha}}^\dagger a_{\bar{\beta}} a_\beta, \quad (1)$$

where α denotes the quantum numbers ($nljm$). The state $\bar{\alpha}$ is the same as α , but with the sign of m reversed. Here S_α is the phase factor $(-1)^{j-m}$. The quadrupole-quadrupole ($q.q$) part of the interaction is given by

$$V_{q.q} = (\chi/2) \sum_{\alpha\beta\gamma\delta} \sum_{\mu} \langle \alpha | q_\mu^2 | \gamma \rangle \langle \beta | q_{-\mu}^2 | \delta \rangle \times (-1)^\mu a_\alpha^\dagger a_\beta^\dagger a_\delta a_\gamma, \quad (2)$$

where the operator q_μ^2 is given by

$$q_\mu^2 = (16\pi/5)^{1/2} r^2 Y_\mu^2(\theta, \phi). \quad (3)$$

The strengths for the like particle neutron-neutron ($n-n$), proton-proton ($p-p$) and neutron-proton ($n-p$) components of the quadrupole-quadrupole ($q.q$) interaction were taken as

$$\chi_{nn} (= \chi_{pp}) = -0.0102 \text{ MeV } b^{-4}$$

and

$$\chi_{np} = -0.0204 \text{ MeV } b^{-4}$$

Here $b (= \sqrt{\hbar/m\omega})$ is the oscillator parameter. These values for the strengths of the $q.q$ interactions compare favorably with the ones employed by Devi et al.[19]. The strength for the pairing interaction was fixed through the approximate relation $G = (18 - 21)/A$. As we have carried out the calculations by incorporating octupole-octupole and hexadecapole-hexadecapole interaction terms in the PQ two body interaction. The forms of higher multipole interaction terms were taken as

$$V_{d.d} = (\chi/2) \sum_{\alpha\beta\gamma\delta} \sum_{\nu=-\lambda}^{\lambda} (-1)^\nu \langle \alpha | d_\nu^\lambda | \gamma \rangle \langle \beta | d_{-\nu}^\lambda | \delta \rangle a_\alpha^\dagger a_\beta^\dagger a_\delta a_\gamma \quad (4)$$

where the operator d_ν^λ is given by

$$d_\nu^\lambda = r^\lambda Y^\lambda_\nu(\theta, \phi). \quad (5)$$

For $\lambda = 3$ and 4, the octupole-octupole and hexadecapole-hexadecapole interaction terms are obtained. The relative magnitudes of the parameters of the octupole-octupole and hexadecapole-hexadecapole parts of the two body interaction were calculated from a relation suggested by Bohr and Mottelson [20]. According to them the approximate magnitude of these constants for isospin $T=0$ is given by

$$\chi_\lambda = \frac{4\pi}{2\lambda + 1} \frac{m\omega_0^2}{A \langle r^{2\lambda-2} \rangle} \text{ for } \lambda = 1, 2, 3, 4... \quad (6)$$

and the parameters for the $T=1$ case are approximately half the magnitude of their $T=0$ counterparts. This relation was used to calculate the values of χ_{pp3} and χ_{pp4} relative to χ_{pp} by generating the wave function for ^{124}Ce and then calculating the values of $\langle r^{2\lambda-2} \rangle$ for $\lambda = 2, 3$ and 4.

The values of these parameters for octupole-octupole interaction work out to be

$$\chi_{pp3} (= \chi_{nn3}) = -0.00366 \text{ MeV } b^{-6}$$

and

$$\chi_{pn3} = -0.00690 \text{ MeV } b^{-6}$$

whereas their values for hexadecapole-hexadecapole part of the two body interaction turn out to be

$$\chi_{pp4} (= \chi_{nn4}) = -0.00020 \text{ MeV } b^{-8}$$

and

$$\chi_{pn4} = -0.00041 \text{ MeV } b^{-8}.$$

II.2 Projection of the states of good angular momentum from axially symmetric HB intrinsic states

The procedure for obtaining the axially symmetric HB intrinsic states has been discussed in reference [21].

The axially symmetric HB states can be written as

$$|\Phi_0\rangle = \prod_{im} (u_i^m + \nu_i^m b_{im}^\dagger b_{im}^\dagger) |0\rangle, \quad (7)$$

where the creation operator b_{im}^\dagger can be expressed as

$$b_{im}^\dagger = \sum_j c_{ji}^m a_{jm}^\dagger, \quad b_{im}^\dagger = \sum_j (-1)^{l+j-m} c_{ji}^m a_{j-m}^\dagger. \quad (8)$$

Here the creation operators a_{jm}^\dagger create a particle in the orbit $|nljm\rangle$ and c_{ji}^m are the expansion coefficients. The index j labels the single-particle states and the index i is employed to distinguish between the different deformed single-particle states with the same $\langle \hat{J}_z \rangle = m$.

The states with good angular momenta J projected from the HB state $|\Phi_K\rangle$ can be written as

$$\begin{aligned} |\Psi_K^J\rangle &= P_{KK}^J |\Phi_K\rangle \\ &= [(2J+1)/8\pi^2] \int D_{KK}^J(\Omega) R(\Omega) |\Phi_K\rangle d\Omega \end{aligned} \quad (9)$$

where $R(\Omega)$ and $D_{KK}^J(\Omega)$ are the rotation operators of the rotation matrix, respectively. The energy of the state with the angular momentum J is given as

$$\begin{aligned} E_J &= \langle \Phi_0 | H P_{00}^J | \Phi_0 \rangle / \langle \Phi_0 | P_{00}^J | \Phi_0 \rangle \\ &= \frac{\int_0^\pi h(\theta) d_{00}^J(\theta) d(\cos\theta)}{\int_0^\pi n(\theta) d_{00}^J(\theta) d(\cos\theta)}, \end{aligned} \quad (10)$$

Here the overlap integrals $h(\theta)$ and $n(\theta)$ are given by

$$\begin{aligned} h(\theta) &= n(\theta) \left[\sum_\alpha \epsilon(\alpha) \rho_{\alpha\alpha} - (G/4) \sum_{\alpha\tau_3} S_\alpha [f(1+M)^{-1}]_{\alpha\bar{\alpha}}^{\tau_3} \sum_{\beta\tau_3} S_\beta [(1+M)^{-1}F]_{\beta\bar{\beta}}^{\tau_3} \right. \\ &\quad \left. - (1/2) \sum_{\tau_3\tau_3'\mu} (-1)^\mu \chi_{\tau_3\tau_3'} \sum_{\alpha\gamma} \langle \alpha | q_\mu^2 | \gamma \rangle \rho_{\alpha\gamma}^{\tau_3} \sum_{\beta\delta} \langle \beta | q_{-\mu}^2 | \delta \rangle \rho_{\delta\beta}^{\tau_3'} \right] \end{aligned} \quad (11)$$

where

$$n(\theta) = \{ \det[1 + M(\theta)] \}^{1/2}, \quad (12)$$

$$F_{\alpha\beta}(\theta) = \sum_{m'_\alpha, m'_\beta} d_{m'_\alpha m'_\alpha}^{j\alpha}(\theta) d_{m'_\beta m'_\beta}^{j\beta}(\theta) f_{j_\alpha m'_\alpha, j_\beta m'_\beta}, \quad (13)$$

$$f_{\alpha\beta} = \sum_i C_{j_\alpha i}^{m_\alpha} C_{j_\beta i}^{m_\beta} \left(\frac{\nu_i^{m_\alpha}}{u_i^{m_\alpha}} \right) \delta_{m_\alpha, -m_\beta}, \quad (14)$$

$$M(\theta) = F(\theta) f^\dagger, \quad (15)$$

$$\rho_{\alpha\beta}(\theta) = \{ M(\theta) / [1 + M(\theta)] \}_{\alpha\beta} = \delta_{\alpha\beta} - \{ [1 + M(\theta)]^{-1} \}_{\alpha\beta}. \quad (16)$$

The yrast energies are calculated as follows. Using the results for the HB calculations - and these are summarized in terms of the amplitudes (u_i^m, ν_i^m) and the expansion coefficients c_{ji}^m - we first set up the (50×50) f -matrix in the present configuration space. Then F , M , and $(1+M)^{-1}$ are computed for 20 Gaussian quadrature points in the range $(0, \pi/2)$. Finally, the projected energies are calculated employing equations (10)-(16).

II.3 The variation-after-angular momentum projection (VAP) method

The VAP calculations has been carried out as follows. We first generated the self-consistent HB solutions, $\phi(\beta)$, by carrying out the HB calculations with the Hamiltonian $(H - \beta Q_0^2)$, where ' β ' is a parameter. The selection of the optimum intrinsic states, $\phi_{\text{opt}}(\beta_J)$, is then made by finding out the minimum of the projected energy

$$E_J(\beta) = \langle \phi_0(\beta) | H P_{00}^J | \phi_0(\beta) \rangle / \langle \phi_0(\beta) | P_{00}^J | \phi_0(\beta) \rangle, \quad (17)$$

as a function of β . In other words, the optimum intrinsic state for each yrast J satisfies the conditions

$$\partial / \partial \beta [\langle \phi_0(\beta) | H P_{00}^J | \phi_0(\beta) \rangle / \langle \phi_0(\beta) | P_{00}^J | \phi_0(\beta) \rangle]_{\beta=\beta_J} = 0, \quad (18)$$

III Deformation systematics of $^{124-132}\text{Ce}$ isotopes

If one looks at the observed E_2^+ energy and E_4^+/E_2^+ values (see Table 1), one observes a systematic increase in the value of E_2^+ energy and a decrease in the E_4^+/E_2^+ values as one moves from ^{124}Ce to ^{132}Ce . It may be noted that $^{124-128}\text{Ce}$ are reasonably well deformed nuclei with E_4^+/E_2^+ values ≥ 3.00 . Within the framework of hydrodynamic model, Bohr and Mottelson [22], have derived a simple expression for the $B(E2)$ values in terms of the transition energy of E_2^+ state. If one analyses the systematics of the E_2^+ energy values in the light of this relation, that may be interpreted to imply that the E_2^+ systematics bear an inverse correlation to the observed quadrupole moment (Q_2^+) systematics. Since the Q_2^+ of a nucleus is directly related to its intrinsic quadrupole moment, the observed systematics of the E_2^+ with A should produce a corresponding inverse systematics of intrinsic quadrupole moments of the neutron-deficient Ce isotopes with increasing 'A'. Based upon the above logic, the calculated values of intrinsic quadrupole moments should exhibit an inverse systematics of the E_2^+ state. Thus, for the neutron - deficient $^{124-132}\text{Ce}$ isotopes, there should be a systematic decrease in the intrinsic quadrupole moments as one moves from ^{124}Ce to ^{132}Ce . The decrease in the quadrupole moment for ^{128}Ce to ^{130}Ce and ^{130}Ce to ^{132}Ce should be large as compared to other Ce isotopes. In Table 1, the results of HB calculations are presented. It may be noted that for the ^{124}Ce , the intrinsic quadrupole moment is $94.50 b^2$, where b is a harmonic oscillator parameter. This value is the largest, meaning thereby that this nucleus should be highly deformed that is what is observed experimentally. For ^{128}Ce to ^{132}Ce , one observes large steps of decrease in intrinsic quadrupole moments as 'A' changes from 128 to 132. The change in intrinsic quadrupole moments is from 91.42 to $77.80 b^2$. For ^{124}Ce to ^{128}Ce , the steps of decrease in the intrinsic quadrupole moments are very slow meaning thereby that there is a slow decrease in the degree of deformation from ^{124}Ce to ^{128}Ce . The trend exhibited by the intrinsic quadrupole moments is therefore seen to be in synchrony with the observed E_2^+ systematics of the neutron-deficient $^{124-132}\text{Ce}$ isotopes.

Attention is next focussed on the factors that are responsible for making the neutron-deficient Ce isotopes to exhibit such features. In this regard, it is important to discuss and highlight some of the well accepted factors responsible for bringing in sizeable collectivity in the nuclei in general. It is well known that if the down slopping components of a high-

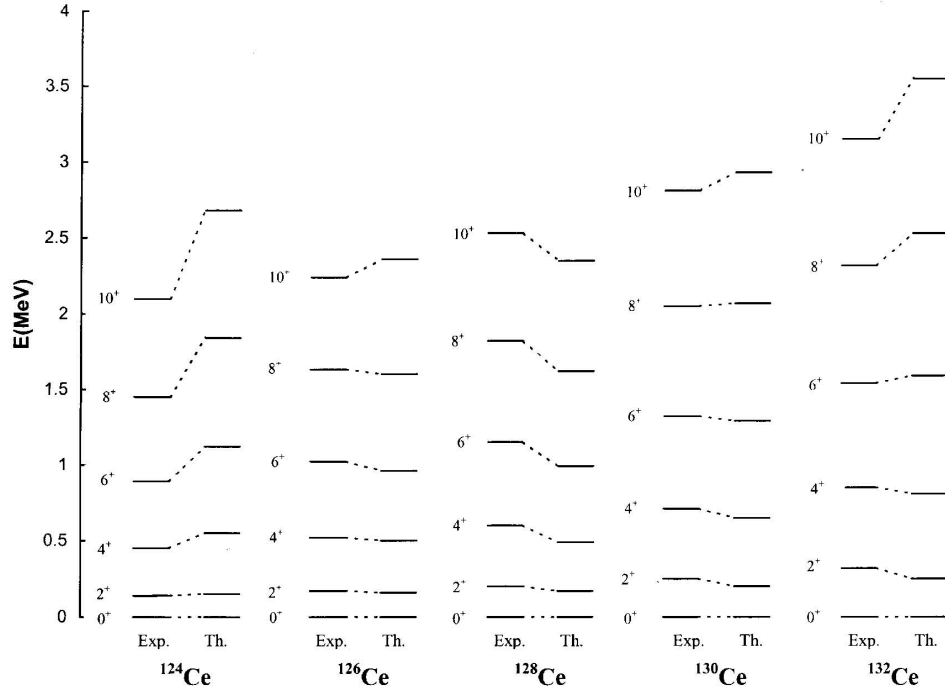
j valence orbit starts filling up, it has the effect of bringing in sharp increase in collectivity. Further, if the higher components of a high- j orbit starts filling up, there would be a slow decrease in collectivity. Besides this, we know that a closed shell or a sub-shell makes zero contribution to the intrinsic quadrupole moment. Therefore, if a sub-shell gets polarized and still has occupation probability greater than the mid sub-shell occupation, then it will again have the effect of introducing some degree of deformation in the nucleus. In the light of above effects, we now try to find out the causes responsible for the observed systematics of neutron-deficient Ce isotopes. In Tables 2 and 3, the results of occupation probabilities of various proton and neutron sub-shells for the ground state, calculated from HB wave function generated for $^{124-132}\text{Ce}$ isotopes are presented. It may be noted from the Table 2 that proton sub-shells $3s_{1/2}$, $2d_{3/2}$, $2d_{5/2}$ and $1h_{11/2}$, have nearly constant value of proton occupation probabilities with increasing 'A'. But the occupation probability of $1g_{7/2}$ proton sub-shell decreases slowly with an increasing value of 'A' for $^{124-132}\text{Ce}$ isotopes. Because of the slow decrease in the $1g_{7/2}$ proton sub-shell occupation probability with 'A', a slow decrease in protonic contribution to intrinsic quadrupole moments is seen to occur as one moves from ^{124}Ce to ^{132}Ce . From Table 3, it is observed that the values of occupation probabilities of $2d_{5/2}$ and $1g_{7/2}$ neutron sub-shells are increasing with increasing mass number A and is more than half full. As the occupation probabilities of $2d_{5/2}$ and $1g_{7/2}$ neutron sub-shells are more than half full and increase with an increase in mass number A , there is a corresponding decrease in the intrinsic quadrupole moments as one goes from ^{124}Ce to ^{132}Ce . Now, coming to the discussion of $h_{11/2}$ neutron orbit occupation probability, one observes from Nilsson diagrams that the slope of $h_{11/2, \pm 5/2}$ orbit is weakly down slopping. As seen from Table 3 the occupation probability of $1h_{11/2}$ neutron orbit increases from a value of 4.16 to 5.75 as we pass from ^{124}Ce to ^{132}Ce . This means that the additional neutrons are filling the weakly down slopping $h_{11/2, \pm 5/2}$ orbit as one moves from ^{124}Ce to ^{132}Ce . This effect also results into a very small change in neutronic contribution to the intrinsic quadrupole moments. Considering the effect of all the factors, the net result is that there is a decrease in the calculated intrinsic quadrupole moments as one moves from ^{124}Ce to ^{132}Ce . From what has been said, the overall observed deformation systematics in $^{124-132}\text{Ce}$ can be understood in terms of the systematic changes in the occupation probabilities of the various valence orbits as explained above.

Table 2. The sub-shell occupation numbers (protons) in the nuclei $^{124-132}\text{Ce}$.

Nucleus	Subshell Occupation Number							
	$3s_{1/2}$	$2d_{3/2}$	$2d_{5/2}$	$2f_{7/2}$	$1g_{7/2}$	$1h_{9/2}$	$1h_{11/2}$	$1i_{13/2}$
^{124}Ce	0.56	1.45	2.60	0.48	1.38	0.00	1.53	0.00
^{126}Ce	0.58	1.48	2.58	0.48	1.36	0.00	1.52	0.00
^{128}Ce	0.58	1.49	2.62	0.47	1.31	0.00	1.53	0.00
^{130}Ce	0.59	1.53	2.66	0.41	1.22	0.00	1.52	0.07
^{132}Ce	0.53	1.45	2.81	0.40	1.21	0.00	1.59	0.01

Table 3. The sub-shell occupation numbers (neutrons) in the nuclei $^{124-132}\text{Ce}$.

Nucleus	Subshell Occupation Number							
	$3s_{1/2}$	$2d_{3/2}$	$2d_{5/2}$	$2f_{7/2}$	$1g_{7/2}$	$1h_{9/2}$	$1h_{11/2}$	$1i_{13/2}$
^{124}Ce	0.97	1.83	4.43	0.91	3.55	0.06	4.16	0.09
^{126}Ce	1.02	1.88	5.04	0.99	4.04	0.01	4.94	0.08
^{128}Ce	1.14	2.03	5.52	0.98	4.90	0.09	5.23	0.11
^{130}Ce	1.52	2.42	5.74	0.94	5.31	0.10	5.85	0.12
^{132}Ce	1.96	3.46	5.91	0.90	5.80	0.10	5.75	0.12

Figure 1. Experimental and theoretical low-lying yrast spectra for the $^{124-132}\text{Ce}$ nuclei (data taken from references [1-10]).

IV Yrast spectra

In Fig. 1, the low-lying yrast spectra of $^{124-132}\text{Ce}$ isotopes is displayed. The experimental yrast energy spectra is seen to be reproduced up to 10^+ with reasonable accuracy. We have also examined the reliability and goodness of the HB wave functions by calculating the $B(E2; 0^+ \rightarrow 2^+)$ values. We have used the rotational model formula [23] for the calculation of $B(E2; 0^+ \rightarrow 2^+)$ transition probabilities from the values of intrinsic quadrupole moments of protons and neutrons. According to this formula

$$B(E2; 0^+ \rightarrow 2^+) = (1.02 \times 10^{-5}) A^{2/3} [e_\pi \langle Q_0^2 \rangle_\pi + e_\nu \langle Q_0^2 \rangle_\nu]^2, \quad (19)$$

where $\langle Q_0^2 \rangle_\pi$ (or $\langle Q_0^2 \rangle_\nu$) are the intrinsic quadrupole moments of valence protons (neutrons) and the proton (neutron) effective charges e_π (e_ν) are

$$e_\pi = (1 + e_{eff}) \quad \text{and} \quad e_\nu = (e_{eff})$$

Table 4. Comparison of the experimental and calculated $B(E2; 0_1^+ \rightarrow 2_1^+)$ values in $^{124-132}\text{Ce}$ isotopes. The $B(E2)$ values are in units of $e^2 \cdot b^2$. Experimental data presented in column 2nd is taken from reference [8].

Nucleus	$B(E2; 0_1^+ \rightarrow 2_1^+) e^2 \cdot b^2$		
	Experimental	Th.	
		$e_{eff} = 0.55$	$e_{eff} = 0.70$
^{124}Ce	3.7(9)	2.17	2.88
^{126}Ce	2.33(14)	2.16	2.87
^{128}Ce	2.16(23)	2.12	2.81
^{130}Ce	2.00(17)	1.96	2.58
^{132}Ce	1.90(30)	1.79	2.34

We have used this formula for the calculation of $B(E2)$ values for the entire isotopic mass chain of neutron-deficient Ce isotopes. In Table 4, we present a comparison of the observed $B(E2; 0_1^+ \rightarrow 2_1^+)$ values with the values calculated

by substituting in relation (19), the values of $\langle Q_0^2 \rangle_\pi$ and $\langle Q_0^2 \rangle_\nu$ for $^{124-132}\text{Ce}$ given in Table 1. It is satisfying to note that the calculated $B(E2)$ value estimates, are in satisfactory agreement with the experimental values for the $0_1^+ \rightarrow 2_1^+$ transition.

V Conclusions

Based upon the results of the present calculations, the following broad conclusions can be drawn.

1. The experimental low-lying systematics, yrast spectra and $B(E2)$ transition probabilities of neutron-deficient $^{124-132}\text{Ce}$ isotopic mass chain are reproduced with reasonable accuracy by using PQOH interaction.
2. The decrease in collectivity as one moves from ^{124}Ce to ^{132}Ce is seen to arise due to the slow decrease in the occupation of $1g_{7/2}$ proton orbit. Besides this, it is found that the $2d_{5/2}$ and $1g_{7/2}$ neutron orbits are more than half full and their occupations increase with an increase in 'A'. This results in the decrease of intrinsic quadrupole moments as one moves from ^{124}Ce to ^{132}Ce .
3. As the slope of the $1h_{11/2, \pm 5/2}$ orbit is weakly down slopping and the occupation probability of this neutron orbit increases as we pass from ^{124}Ce to ^{132}Ce , the additional neutrons are found to be filling this orbit resulting into a very small change in neutronic contribution to the intrinsic quadrupole moments.

References

- [1] G.S. Li, Z.Y. Dai, S.X. Wen, S.G. Li, P.K. Weng, I.K. Zhang, G.J. Yuan, and C.X. Yang, *Z. Phys. A* **356**, 119 (1996).
- [2] D.M. Todd, R. Aryaeinejad, D.J.G. Love, A.H. Nelson, P.J. Nolan, P.J. Smith, and P.J. Twin, *J. Phys. G* **10**, 1407 (1984).
- [3] J.C. Wells, N.R. Johnson, J. Hattula, M.P. Fewell, D.R. Haenni, I.Y. Lee, F.K. Mc Gowan, J.W. Johnson, and L.L. Riedinger, *Phys. Rev. C* **30**, 1532 (1984).
- [4] P.J. Nolan, D.M. Todd, P.J. Smith, D.J.G. Love, P.J. Twin, O. Andersen, J.D. Garrett, G.B. Hagemann, and B. Herskind, *Phys. Lett. B* **108**, 269 (1982).
- [5] D. Ward, H. Hertschat, P.A. Butler, P. Colombani, R.M. Diamond, and F.S. Stephens, *Phys. Lett. B* **56**, 139 (1975).
- [6] Yu. V. Sergeenkov, *Nucl. Data Sheets* **58**, 795 (1989).
- [7] M.R. Bhat et al., *Nucl. Data Sheets* **80**, 1060 (1997).
- [8] S. Raman, C.H. Malarkey, C.W. Nester Jr., and P. Tikkanen, *At. Data Nucl. Data Tables* **76**, 69 (2001).
- [9] C.J. Lister, B.J. Varley, R. Moscrop, W. Gelletly, P.J. Nolan, et al., *Phys. Rev. Lett.* **55**, 810 (1985).
- [10] M. Sakai, *At. Data, Nucl. Data Tables* **31**, 415 (1984).
- [11] J.-Y. Zhang, R.F. Casten, and N.V. Zamfir, *Phys. Rev. C* **48**, R10 (1993).
- [12] J. Yan, O. Vogel, P. von Brentano, and A. Gelberg, *Phys. Rev. C* **48**, 1046 (1993).
- [13] N. Onishi and Y. Yoshida, *Nucl. Phys.* **80**, 367 (1966).
- [14] M. Baranger, *Phys. Rev. C: Nucl. Phys.* **130**, 1244 (1963).
- [15] J.D. Vergados and T.T.S. Kuo, *Phys. Lett. B* **35**, 93 (1971).
- [16] P. Federman, S. Pittel, and R. Compos, *Phys. Lett. B* **82**, 9 (1989).
- [17] S.G. Nilsson and I. Ragnarsson, *Shapes and Shells in Nuclear Structure* (Cambridge Univ. press, 1995) p.122.
- [18] M. Baranger and K. Kumar, *Nucl. Phys. A* **110**, 490 (1968).
- [19] R. Devi, S.P. Saraswat, A. Bharti, and S.K. Khosa, *Phys. Rev. C* **55**, 2433 (1997).
- [20] A. Bohr and B.R. Mottelson, *Nuclear Structure* (Benjamin Reading, MA, 1975), Vol. II, p. 356.
- [21] S.K. Sharma, *Nucl. Phys. A* **260**, 226 (1976).
- [22] A. Bohr and B.R. Mottelson, *Mat. Fys. Medd. Dan. Vid. Selsk.* **27**, no. 16 (1953).
- [23] G. Ripka, *Adv. in Nucl. Phys.*, edited by M. Baranger and E. Vogt, (Plenum, New York, 1968) Vol. 1. C.G. Adler, M.K. Banerjee and G.J. Stephenson, Jr *Bull Am Phys. Soc.* **13**, 581 (1968).